

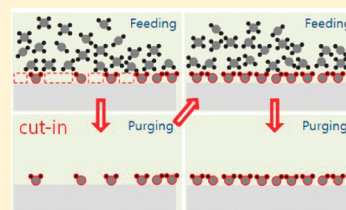
# Improved Growth and Electrical Properties of Atomic-Layer-Deposited Metal-Oxide Film by Discrete Feeding Method of Metal Precursor

Tae Joo Park,<sup>†</sup> Jeong Hwan Kim, Jae Hyuck Jang, Un Ki Kim, Sang Young Lee, Joohwi Lee, Hyung Suk Jung, and Cheol Seong Hwang\*

WCU Hybrid Materials Program, Department of Materials Science and Engineering and Inter-university Semiconductor Research Center, Seoul National University, Seoul, 151-744, Korea

**ABSTRACT:** A new model for the growth behavior of saturated HfO<sub>2</sub> films by atomic layer deposition (ALD) was suggested. The well-known ALD saturation of the growth rate with increasing precursor input was observed, but the full saturation required an extremely long feeding time. After the rapid increase in growth rate with increasing precursor feeding time, a pseudo-saturation region was observed where full saturation was hindered by the “screening effect” of the physisorbed precursor molecules or byproduct molecules on the chemisorbed species. The physisorbed precursor molecules screen the active adsorption sites for the following precursor. The discrete feeding method, which is the modified process recipe suggested in this study, provided improved growth behavior and electrical properties of the film.

**KEYWORDS:** ALD, HfO<sub>2</sub>, growth rate



## I. INTRODUCTION

Atomic layer deposition (ALD) is one of the most promising methods for nanoscale thin film deposition for the fabrication of electronic devices and nanostructured materials.<sup>1–3</sup> The ALD growth of metal-oxide film is based on the ligand exchange reaction (surface reaction) between the precursor and oxygen source molecules. In general, the growth rate of the ALD film increases as the feeding time of the metal precursor in the subsaturation region increases, and it appears to saturate at a certain feeding time when the precursor dose is sufficiently high to completely cover the active sites on the film (or substrate) surface. This point is generally considered to be the growth-saturated feeding time (growth-saturated ALD condition). One important factor that affects the saturated growth rate of the ALD film is the steric hindrance caused by the physical size and proximity of the neighboring parts of the precursor (or partially decomposed) molecule during precursor feeding.<sup>4,5</sup> It is also probable that reaction byproduct molecules screen the adsorption site, which also impedes the active chemical adsorption of precursor molecules. Figure 1a gives a representative example of this phenomenon, which shows the nominal growth rate (film thickness divided by the ALD cycle number, 30) of the HfO<sub>2</sub> films grown at 250 °C using Hf[N(CH<sub>3</sub>)<sub>2</sub>]<sub>4</sub> (TDMAHf), Hf[N(CH<sub>3</sub>)(C<sub>2</sub>H<sub>5</sub>)]<sub>4</sub> (TEMAHf), and Hf[N(C<sub>2</sub>H<sub>5</sub>)<sub>2</sub>]<sub>4</sub> (TDEAHf), as a function of the Hf-precursor feeding time. O<sub>3</sub>, at a concentration of 150 g/Nm<sup>3</sup>, was used as the oxygen source. The film thickness includes the interfacial layer thickness, (~1–1.5 nm), which means that the absolute growth rates shown in Figure 1a have low importance. The growth rates for all cases appear to be saturated over a Hf precursor feeding time of 3 s. The saturated growth rate is highest and lowest in the case of TDMAHf and TDEAHf, respectively. When the precursor

molecules cover the film (or substrate) surface, the number of Hf ions on the surface is inversely proportional to the physical size of the precursor molecule. Therefore, the growth rate of a HfO<sub>2</sub> film grown using TDMAHf and TDEAHf, which has a smallest and largest precursor molecule size,<sup>6</sup> shows a highest and lowest (saturation) growth rate, respectively. This already shows the importance of considering the steric hindrance effect caused by the size of the precursor molecules. However, the denser chemical adsorption (chemisorption) of the precursor molecule is affected by not only these factors but also the “screening effect”, which is considered to be a type of steric hindrance effect. The screening effect means that the overlying physically adsorbed (physisorbed) precursor molecules on the chemisorbed precursor molecule layer, which was formed during the initial period of precursor feeding step could screen the unoccupied active sites on the surface for the subsequent precursor molecules during the later period of the precursor feeding step. In this study, the detailed mechanism of the screening effect and its effect on the growth behavior of ALD films were suggested and discussed. In addition, a “discrete feeding method” (DFM) of the metal precursor was proposed as a solution for improved film growth. The electrical properties of the various films were also examined.

## II. EXPERIMENTAL PROCEDURE

ALD HfO<sub>2</sub> thin films were grown on a RCA-cleaned *p*-type Si (100) substrate using an 8-in.-diameter scale traveling-wave-type reactor (Quoros Co., Ltd., Model Plus-200). The substrate temperature was maintained at 250 °C, which is within the safe ALD temperature window. TEMAHf and

**Received:** March 30, 2010

**Revised:** December 5, 2010

**Published:** March 14, 2011

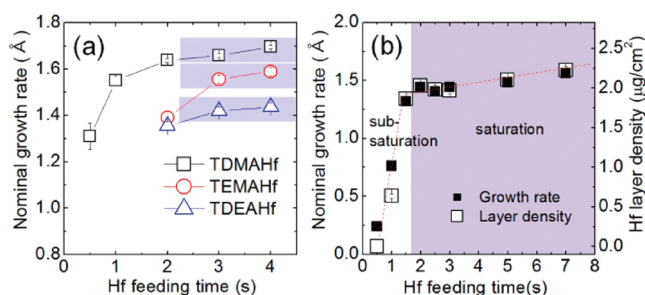


**Figure 1.** (a) Nominal growth rate of the  $\text{HfO}_2$  films grown with TDMAHf, TEMAfh, and TDEAHf, as a function of the Hf-precursor feeding time; (b) nominal growth rate and Hf layer density of the  $\text{HfO}_2$  films grown with TEMAfh, as a function of the Hf-precursor feeding time.

$\text{O}_3$ , at concentrations of  $150 \text{ g/Nm}^3$ , were used as the metal precursor and oxygen source, respectively. TDMAHf and TDEAHf were also used, for comparison. Ultrahigh-purity argon (99.9999%) at a flow rate of 200 standard cubic centimeters per min (sccm) was used as the carrier and purge gas. The Hf-precursor feeding time was varied. The purge after Hf-precursor feeding,  $\text{O}_3$  feeding, and purge time after  $\text{O}_3$  injection were 20, 3, and 20 s, respectively.

The thickness and Hf layer density of the  $\text{HfO}_2$  film were measured by ellipsometry and X-ray fluorescence (XRF), respectively. Post-deposition annealing (PDA) of the selected films for the electrical measurements was performed by rapid thermal annealing at  $760^\circ$  and  $1000^\circ \text{C}$  for 30 s under a  $\text{N}_2$  atmosphere. Electron-beam evaporated platinum was deposited as the top electrode through a shadow mask to fabricate the metal–oxide–semiconductor (MOS) capacitors. Forming gas annealing (FGA) was performed at  $400^\circ \text{C}$  for 30 min in an atmosphere containing 95%  $\text{N}_2$ /5%  $\text{H}_2$  after forming the platinum top electrode. The capacitance–voltage ( $C$ – $V$ ), and gate leakage current–voltage ( $J_g$ – $V$ ) measurements were examined using a Hewlett–Packard Model HP 4194 impedance analyzer and a Hewlett–Packard Model HP 4140B picoammeter/dc voltage source, respectively. The equivalent oxide thickness (EOT) was calculated from the accumulation capacitance measured at 1 MHz, considering the quantum mechanical effect.<sup>7</sup>

### III. RESULTS AND DISCUSSION

**III-A. Growth Behavior of  $\text{HfO}_2$  Film (Pseudo- and Full-Saturation).** Although the growth rate of the ALD film usually appeared to become saturated with increasing precursor feeding time, the growth rate still increased slightly with increasing feeding time, even after the apparent growth-saturated feeding time. Figure 1b shows the nominal growth rate and Hf layer density measured by XRF of the  $\text{HfO}_2$  films with 30 ALD cycles, as a function of the Hf-precursor (TEMAfh) feeding time ( $t_{\text{Hf}}$ ). Although the  $t_{\text{Hf}}$  of 1.5–2 s appeared to be a growth saturation point, the growth rate increased slightly and was not saturated completely, even for  $t_{\text{Hf}} > 7$  s. The Hf layer density showed a similar trend with the growth rate, which means that the incompletely saturated growth behavior of the film was barely affected by Si diffusion into the film and interfacial  $\text{SiO}_2$  layer growth during ALD. The growth rate of the film was eventually saturated completely over a period of  $t_{\text{Hf}} = 12$  s, as shown in Figure 2a. The same growth behavior was observed in the films grown on a Pt substrate.<sup>8,9</sup> Although the growth behavior of the ALD film was conventionally divided into two regions, i.e., subsaturation (0–2 s) and saturation ( $> 2$  s), the saturation region could be divided again into a pseudo- (2–13 s) and

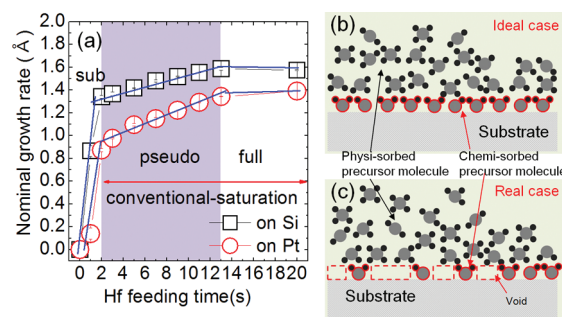


**Figure 2.** (a) Nominal growth rate of the  $\text{HfO}_2$  films grown on Si and Pt substrates, as a function of the Hf-precursor feeding time. (b) Schematic diagram of precursor molecule behavior in the ideal case. (c) Schematic diagram of precursor molecule behavior in the real case.

full-saturation region ( $> 13$  s). In the pseudo-saturation region, the growth rate still increased with increasing Hf-precursor feeding time, even though the increasing rate was much lower than that in the subsaturation region. Eventually, the growth rate was completely saturated in the full-saturation region. Figure 2b shows a schematic diagram for the situation where the chemical adsorption sites are fully covered with chemisorbed precursor molecules during the ALD process. The physically adsorbed molecules on top of the chemisorbed species do not interfere with the ALD reaction. This corresponds to an ideal ALD reaction. The packing density of the chemisorbed precursor molecules should be high on the reactive surface (film or substrate), as shown in Figure 2b, when a sufficient dose of precursor molecules was provided. In this case, the physisorbed precursors do not interact with the surface because the surface adsorption sites are fully covered by the chemisorbed molecules. However, the real case might be quite different from the ideal case, as shown in Figure 2c, where a more realistic situation is depicted.

When the precursor molecules are injected onto the surface, some of them react chemically with the surface sites via the ALD-type ligand exchange reaction. At the same time, several other physicochemical side reactions occur, which adversely interfere with the ALD reaction. When there are some unoccupied active sites for the chemisorption of precursor molecules on the surface with a similar size to the precursor molecule, the overlying physisorbed precursor molecules may screen the remaining active sites from being chemisorbed by subsequent precursor molecules during the feeding step. The thermal energy may not be sufficient to remove the screening molecules and expose the unoccupied sites to the precursor molecules within a short amount of time. Furthermore, the byproduct molecules, such as  $\text{CO}_2$ ,  $\text{H}_2\text{O}$ ,  $\text{CH}_2\text{O}$ , and  $\text{NO}_x$ , etc., which are generated by the reaction of precursor molecules with the surface active site (hydroxyls) during the feeding step of precursor,<sup>12</sup> can also screen the remaining active sites, just like the overlying physisorbed precursor molecules. Therefore, after the purging step, which blows out the overlying physisorbed precursor molecules or byproduct molecules on the chemisorbed precursor layer, a certain number of active sites remain unoccupied when  $t_{\text{Hf}}$  is not long enough.

All these factors make the attainment of a fully saturated ALD rate difficult, and an excessively long precursor feeding time is necessary to achieve it. Amine-based Hf molecules partly decompose thermally at the growth temperature, which may facilitate

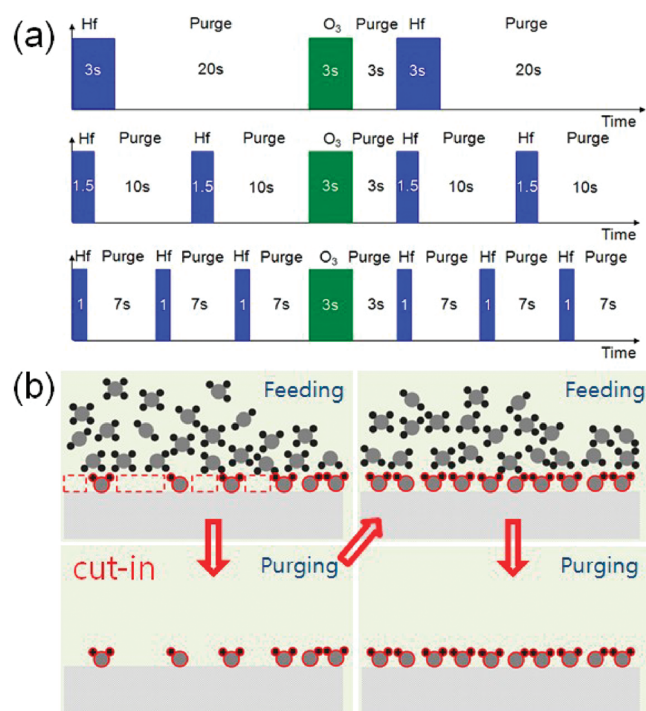


**Figure 3.** (a) Schematic diagram of the DFM process sequence (recipe), and (b) film growth behavior model of the DFM process.

the process of obtaining full saturation by reducing their molecular size. However, it is still rather difficult to achieve the fully saturated growth rate as shown in Figures 1 and 2a. The fully saturated ALD growth behavior suggests that the precursor molecules are not completely thermally decomposed at the ALD temperature.<sup>10,11</sup> The full growth saturation over a period of  $t_{\text{Hf}} = 13$  s in Figure 2a suggests that a chemical vapor deposition (CVD) reaction was not involved in the pseudo-saturation behavior, because a CVD reaction would increase the growth rate continuously as  $t_{\text{Hf}}$  increases without full saturation. In addition, the fact that no film growth occurs without O<sub>3</sub> pulse steps supports that no CVD reaction occurs. Kukli et al. and Hausmann et al. also verified the self-limiting growth of ALD HfO<sub>2</sub> films without the thermal decomposition of precursor molecules at a growth temperature of 250 °C using similar precursors.<sup>10,11</sup> Although the time-dependent rearrangement or decomposition of precursor molecules (ligand release) might be considered as the origin of this pseudo-saturation behavior,<sup>13</sup> this model cannot appropriately explain the experimental results here, which is discussed later in Figure 4.

The formation of a multilayered physisorbed layer could be confirmed from the fact that the deposition rate increased considerably when decreasing the purging time to <5 s. Here, the contribution of the gas phase reaction is negligible, because the gas-phase precursor molecules would be removed even with the purging time of 5 s, considering the pumping capacitance (over 1000 L/min), the inner diameter of exhaust tubing (40 mm), and the reactor volume (8-in. scale traveling wave type). Therefore, the increased growth rate of the film with decreasing purging time supports the formation of the multilayered physisorbed layer during feeding step.

The chance for precursor molecules with sufficient thermal energy to move into the unoccupied active sites and be absorbed

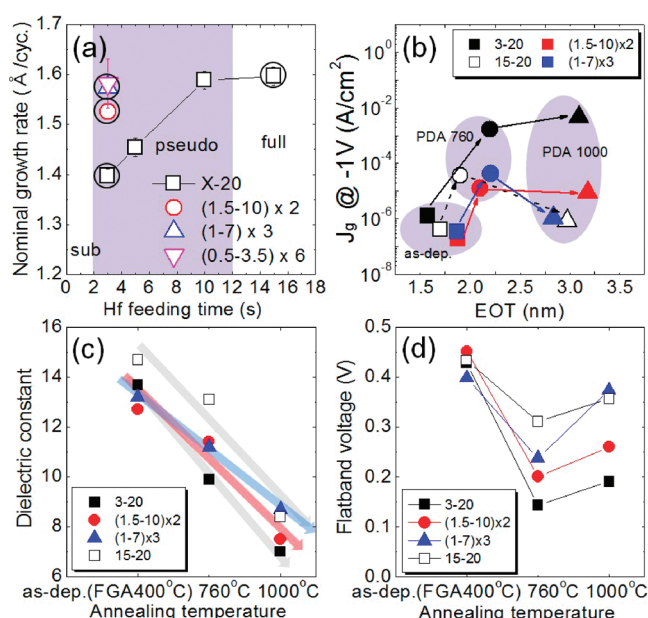


**Figure 4.** (a) Nominal growth rate of the HfO<sub>2</sub> films grown with the conventional and DFM processes, as a function of  $t_{\text{Hf}}$ ; (b) plot of EOT vs  $J_g$  for the selected HfO<sub>2</sub> films; and variations in (c) dielectric constant and (d) flatband voltage of the HfO<sub>2</sub> films, as a function of annealing temperature.

chemically increases with increasing  $t_{\text{Hf}}$ . In this way, the surface coverage of chemisorbed precursor molecules per cycle increases. This results in a gradual increase in the overall growth rate of the film with increasing  $t_{\text{Hf}}$  until full coverage of all possible chemisorption sites is achieved.

**III—B. The Discrete Feeding Method.** Such a long precursor feeding time for full saturation is undesirable, considering the throughput, material consumption, and maintenance of the system. Therefore, an efficient way of achieving full saturation in a shorter time was suggested based on the growth behavior discussed above. The physisorbed precursor molecules or by-product molecules, which screen the underlying active sites, should be removed during the precursor feeding step by a *cut-in* purge step. In the suggested process, the precursor feeding/purge step in the pseudo-saturation region was divided into several shorter feeding/purge steps but with an identical total feeding/purge time (called the *Discrete Feeding Method*, DFM). The conventional process sequence of 3 s (TEMAHf) – 20 s (purge) was divided into 1.5 s (TEMAHf) – 10 s (purge) – 1.5 s (TEMAHf) – 10 s (purge) and 1 (TEMAHf) – 7 (purge) – 1 (TEMAHf) – 7 (purge) – 1 (TEMAHf) – 7 s (purge), as shown in Figure 3a. Figure 3b shows the behavior of the schematic precursor molecules during the Hf-precursor feeding step in the suggested DFM process. The physisorbed precursor molecules or byproduct molecules on the chemisorbed precursor molecules were removed by the *cut-in* purge. Therefore, the active sites (voids) on the surface opened and could be filled effectively with precursor molecules in the following shorter feeding step, which would result in full saturation without the wasteful consumption of the precursor.

The effect of the suggested DFM on the growth rate was confirmed experimentally, as shown in Figure 4. While the nominal growth rate of the film grown using the conventional technique ( $t_{\text{Hf}} = 3$  s and purge time = 20 s) was  $\sim 1.40$  Å/cycle,



that of the film grown using the DFM process  $[(1.5 - 10 \text{ s}) \times 2$  and  $(1 - 7 \text{ s}) \times 3]$  increased to  $\sim 1.53$  and  $\sim 1.57$  Å/cycle, respectively. These values are close to the full-saturated growth rate of  $\sim 1.60$  Å/cycle at  $t_{\text{Hf}} = 15$  s. Even though the amount of injected Hf-precursor molecules is the same with conventional processes, the DFM process increased the growth rate of film. This confirmed again that the chemical vapor deposition (CVD) reaction is hardly involved in the growth of the film.

The growth rate of the film by another DFM scheme of  $[(0.5 - 3.5 \text{ s}) \times 6]$  was also included in Figure 4a to confirm that the probable effects of the time-dependent ligand rearrangement/removal model<sup>13</sup> does not explain the increased growth rate of the DFM process. The growth rates of the films grown by the DFM schemes of  $[(1 - 7 \text{ s}) \times 3]$  and  $[(0.5 - 3.5 \text{ s}) \times 6]$  were almost identical, while being certainly lower for the  $[(1.5 - 10 \text{ s}) \times 2]$  scheme. In the time-dependent ligand rearrangement/removal model,<sup>13</sup> the total available time for the precursors to react (here, 3 s for total pulse time or 23 s for total pulse and purge time) decides the growth rate, even for the same precursor dose. Here, the total exposure time and precursor dose were identical but the growth rate was different, suggesting that the time-dependent ligand rearrangement/removal model cannot explain the experimental results. The almost identical growth rates between the DFM schemes of  $[(1 - 7 \text{ s}) \times 3]$  and  $[(0.5 - 3.5 \text{ s}) \times 6]$  can be explained by the growth model suggested in this study. The feeding times of 1 s, as well as 0.5 s, are in the subsaturation region, which means that a multilayered physisorbed layer is hardly formed in both cases, and, thus, there should be no benefit from extra *cut-in* purge steps. It can be argued that, since the growth rate of 1.57 Å/cycle for the two cases is already close to that of the fully saturated growth rate, there should be no further increase in the growth rate when changing the DFM schemes from  $[(1 - 7 \text{ s}) \times 3]$  to  $[(0.5 - 3.5 \text{ s}) \times 6]$ . However, the full saturation growth rate was 1.60 Å/cycle, which is certainly larger than 1.57 Å/cycle. It should be noted that the increase in the growth rate observed when changing the DFM schemes from  $[(1.5 - 10 \text{ s}) \times 2]$  to  $[(1 - 7 \text{ s}) \times 3]$  was only 0.04 Å/cycle. It should also be noted that the pulse time of 1.5 s is the starting point where the multilayer physisorbed layer begins to form (Figure 1b), which is where the *cut-in* purge steps start to play a role in increasing the growth rate.

**III–C. Electrical Properties of HfO<sub>2</sub> Films.** The electrical properties of the selected films were examined to confirm the effect of DFM on the electrical properties of the film. The films grown using the DFM process  $[(1.5 - 10 \text{ s}) \times 2$  and  $(1 - 7 \text{ s}) \times 3]$  and the conventional technique at the beginning of the pseudo-saturation region (3 s) and full-saturation region (15 s) were used to evaluate the electrical properties. Figure 4b shows a plot of EOT vs  $J_g$  for the selected HfO<sub>2</sub> films before and after PDA. PDA at high temperatures generally degrades the electrical performance of the films.<sup>14–17</sup> The EOT and  $J_g$  increased due to the crystallization of the film and interfacial layer growth during PDA, which were suppressed significantly in the film grown with  $t_{\text{Hf}} = 15$  s, compared to the film grown with  $t_{\text{Hf}} = 3$  s. The film showed a  $\sim 2$ - and  $\sim 4$ -order-of-magnitude decrease in  $J_g$  after PDA at 760 and 1000 °C, respectively, despite the smaller EOT. It was reported previously that the  $J_g$  of the HfO<sub>2</sub> film increased after PDA at 760 °C, because of the crystallization of the film, but decreased after PDA at 1000 °C, because of the overwhelming growth of the interfacial layer.<sup>14,18</sup> Akbar et al. reported that the increased  $t_{\text{Hf}}$  might enhance Hf coverage, resulting in reduced vacancies and improved overall bonding strength in the film.<sup>19</sup>

Therefore, the increased feeding time makes the film chemically and electronically more solid, thereby improving the thermal stability of the film. The films grown using the DFM process showed improved properties, compared to those with a Hf-precursor feeding time of 3 s, despite the same (total) feeding time, which is similar to those with a Hf-precursor feeding time of 15 s. This suggests that the DFM improved not only the growth behavior (faster growth saturation) but also the electrical properties (thermal stability) of the film, because of the solid chemical and electronic structure.

Figure 4c shows the changes in the dielectric constant of the HfO<sub>2</sub> films, as a function of annealing temperature. The effective dielectric constant was estimated using a single sample so the contribution from the interfacial layer would be included. The dielectric constant of all the films decreased as the PDA temperature increased, which is indicated by the arrows. This is more evident when the films were grown with the conventional process in the subsaturation region. However, this degradation was retarded by using the DFM process. Eventually, the dielectric constant of the film grown using the DFM process of  $[(1 - 7 \text{ s}) \times 3]$  after PDA at 1000 °C was similar to that of the film grown using the conventional process with  $t_{\text{Hf}} = 15$  s. It is expected that the higher physical and chemical density of the film, which was induced by the DFM process, increases the dielectric constant,<sup>20</sup> as well as the thermal stability. This is a very positive result, considering that only one-fifth of the Hf-precursor feeding is used in the DFM, compared to the conventional process.

Figure 4d shows the changes in flatband voltage ( $V_{\text{FB}}$ ) values of the various films, as a function of annealing temperature.  $V_{\text{FB}}$  shifts generally reflect the fixed charge status of the film near the interface with Si, which is induced by the interfacial chemical structure. Therefore, the smaller changes in the  $V_{\text{FB}}$  values after PDA of the films grown conventionally with  $t_{\text{Hf}} = 15$  s suggest the better thermal stability of this process, compared to a film grown with  $t_{\text{Hf}} = 3$  s. The  $V_{\text{FB}}$  behavior of the films grown using the DFM process became closer to the conventional film with  $t_{\text{Hf}} = 15$  s as the number of *cut-in* cycles increased, which confirms that the DFM process improves the thermal stability of the film.

## IV. CONCLUSIONS

In summary, the saturation behavior of ALD HfO<sub>2</sub> films was observed carefully, and new model for the film growth behavior was suggested. The slight increase in the growth rate of the film with increasing Hf-precursor feeding time, even after the conventional saturation point was reached, was explained by a “screening effect”, where the physisorbed precursor molecules or byproduct molecules on the chemisorbed screen the active sites for the following precursor. The discrete feeding method to improve the growth behavior was proposed, based on the suggested growth behavior modeling, and verified. The fully saturated growth rate at a much shorter precursor feeding time and improved electrical properties of the film could be obtained using the discrete feeding method without excessive consumption of the precursor.

## AUTHOR INFORMATION

### Corresponding Author

\*E-mail: cheolsh@snu.ac.kr.

### Present Addresses

<sup>†</sup>Department of Materials Engineering, Hanyang University, Ansan, 426-791, Korea.

## ■ ACKNOWLEDGMENT

The study was supported by the Converging Research Center Program through the National Research Foundation of Korea (NRF) funded by the Ministry of Education, Science and Technology (2010K000977), the IT R&D program of MKE/KEIT [KI002178, Development of a mass production compatible capacitor for next generation DRAM], and WCU (World Class University) program through National Research Foundation of Korea funded by the Ministry of Education, Science and Technology (R31-2008-000-10075-0).

## ■ REFERENCES

- (1) Suntola, T. *Mater. Sci. Rep.* **1989**, *4*, 261.
- (2) George, S. M. *Chem. Rev.* **2010**, *110*, 111.
- (3) Park, T. J.; Kim, J. H.; Jang, J. H.; Na, K. D.; Hwang, C. S.; Kim, J. H.; Kim, G.-M.; Choi, J. H.; Choi, K. J.; Jeong, J. H. *Appl. Phys. Lett.* **2007**, *91*, 252106.
- (4) Alam, M. A.; Green, M. L. *J. Appl. Phys.* **2003**, *94*, 3403.
- (5) Ylilammi, M. *Thin Solid Films* **1996**, *279*, 124.
- (6) Hackley, J. C.; Demaree, J. D.; Gougousia, T. *J. Vac. Sci. Technol. A* **2008**, *26*, 5.
- (7) Connelly, D.; Yu, Z.; Yergeau, D. *IEEE Trans. Electron Devices* **2002**, *49*, 4.
- (8) Han, J. H.; Lee, S. W.; Choi, G.-J.; Lee, S. Y.; Hwang, C. S.; Dussarrat, C.; Gatineau, J. *Chem. Mater.* **2009**, *21*, 207.
- (9) Lee, S. S.; Baik, J. Y.; An, K.-S.; Suh, Y. D.; Oh, J.-H.; Kim, Y. *J. Phys. Chem. B* **2004**, *108*, 15128.
- (10) Kukli, K.; Ritala, M.; Sajavaara, T.; Keinonen, J.; Leskela, M. *Chem. Vap. Deposition* **2002**, *8*, 5.
- (11) Hausmann, D. M.; Kim, E.; Becker, J.; Gordon, R. *Chem. Mater.* **2002**, *14*, 4350.
- (12) Liu, X.; Ramanathan, S.; Longdergan, A.; Srivastava, A.; Lee, E.; Seidel, T. E.; Barton, J. T.; Pang, D.; Gordon, R. G. *J. Electrochem. Soc.* **2005**, *152*, G213.
- (13) Jeong, W. G.; Menu, E. P.; Dapkus, P. D. *Appl. Phys. Lett.* **1989**, *55*, 244.
- (14) Park, T. J.; Kim, J. H.; Seo, M. H.; Jang, J. H.; Hwang, C. S. *Appl. Phys. Lett.* **2007**, *90*, 152906.
- (15) Park, J.; Park, T. J.; Cho, M.; Kim, S. K.; Hong, S. H.; Kim, J. H.; Seo, M.; Hwang, C. S.; Won, J. Y.; Jeong, R.; Choi, J.-H. *J. Appl. Phys.* **2006**, *99*, 094501.
- (16) Park, J.; Cho, M.; Kim, S. K.; Park, T. J.; Lee, S. W.; Hong, S. H.; Hwang, C. S. *Appl. Phys. Lett.* **2005**, *86*, 112907.
- (17) Park, T. J.; Kim, J. H.; Jang, J. H.; Na, K. D.; Hwang, C. S.; Yoo, J. H. *J. Appl. Phys.* **2008**, *104*, 054101.
- (18) Park, T. J.; Kim, J. H.; Jang, J. H.; Na, K. D.; Hwang, C. S.; Yoo, J. H. *Electrochem. Solid-State Lett.* **2008**, *11*, H121.
- (19) Akbar, M. S.; Lee, J. C.; Moumen, N.; Peterson, J. *Appl. Phys. Lett.* **2006**, *88*, 082901.
- (20) Park, T. J.; Chung, K. J.; Kim, H. C.; Ahn, J.; Wallace, R. M.; Kim, J. *Electrochem. Solid-State Lett.* **2010**, *13*, G65.